

**Methane variations  
on orbital timescales:  
a transient modeling  
experiment**

T. Y. M. Konijnendijk et al.

# Methane variations on orbital timescales: a transient modeling experiment

T. Y. M. Konijnendijk<sup>1</sup>, S. L. Weber<sup>2,3</sup>, E. Tuenter<sup>1,3</sup>, and M. van Weele<sup>3</sup>

<sup>1</sup>Department of Earth Sciences, Faculty of geosciences, Utrecht University, Budapestlaan 4, 3584 CD Utrecht, The Netherlands

<sup>2</sup>Department of Physical Geography, Faculty of geosciences, Utrecht University, Heidelberglaan 2 3584 CS Utrecht, The Netherlands

<sup>3</sup>KNMI – Royal Netherlands Meteorological Institute, Wilhelminalaan 10, 3732 GK De Bilt, The Netherlands

Received: 12 December 2010 – Accepted: 22 December 2010 – Published: 6 January 2011

Correspondence to: T. Y. M. Konijnendijk (konijnendijk@geo.uu.nl)

Published by Copernicus Publications on behalf of the European Geosciences Union.

Title Page

Abstract

Introduction

Conclusions

References

Tables

Figures

⏪

⏩

◀

▶

Back

Close

Full Screen / Esc

Printer-friendly Version

Interactive Discussion



## Abstract

Methane (CH<sub>4</sub>) variations on orbital timescales are often associated with variations in wetland coverage, most notably in the summer monsoon areas of the Northern Hemisphere. Here we test this assumption by simulating orbitally forced variations in global wetland emissions, using a simple wetland distribution and CH<sub>4</sub> emissions model that was coupled off-line to a climate model containing atmosphere, ocean and vegetation components. The transient climate modeling simulation extends over the last 650 000 yrs and includes variations in land-ice distribution and greenhouse gases. Tropical temperature and global vegetation are found to be the dominant controls for global CH<sub>4</sub> emissions and thus atmospheric concentrations. The relative importance of wetland coverage, vegetation coverage, and emission temperatures depends on the specific climatic zone (boreal, tropics and Indian/Asian monsoon area) and timescale (precession, obliquity and glacial-interglacial timescales).

Simulated variations in emissions agree well with those in measured concentrations, both in their time series and spectra. The simulated lags with respect to the orbital forcing also show close agreement with those found in measured data, both on the precession and obliquity timescale. We only find covariance between monsoon precipitation and CH<sub>4</sub> concentrations, however we find causal links between atmospheric concentrations and tropical temperatures and global vegetation. The primary importance of these two factors explains the lags found in the CH<sub>4</sub> record from ice cores.

## 1 Introduction

As a greenhouse gas, methane (CH<sub>4</sub>) is a forcing factor for climate (Wang et al., 1996). Vice versa, methane concentrations are also subjected to climate changes via changes in natural CH<sub>4</sub> production rate. The most important natural source of CH<sub>4</sub> is anaerobic decomposition of organic material in wetlands (Fung et al., 1991). Global wetland extent, together with more local factors influencing CH<sub>4</sub> production and release such

CPD

7, 47–77, 2011

## Methane variations on orbital timescales: a transient modeling experiment

T. Y. M. Konijnendijk et al.

Title Page

Abstract

Introduction

Conclusions

References

Tables

Figures

⏪

⏩

◀

▶

Back

Close

Full Screen / Esc

Printer-friendly Version

Interactive Discussion



as temperature and vegetation (Gedney et al., 2004), is therefore key to understanding variations in the atmospheric CH<sub>4</sub> concentration in the period before anthropogenic influences.

Variations in CH<sub>4</sub> concentration have been substantial during the late Quaternary. Spahni et al. (2005) found an increase in the Epica Dome C (EDC) ice core record of ~360 parts per billion by volume (ppbv) to ~690 ppbv during the transition from Last Glacial Maximum (LGM; 21 000 yrs before present) to the Early Holocene. Long-term oscillations in the CH<sub>4</sub> record have been linked to variations in insolation caused by orbital forcing, particularly to the 23 000 yr (23-kyr) precession component (e.g. Ruddiman and Raymo, 2003). Strong 41-kyr and 100-kyr components are apparent also in the record (Loulergue et al., 2008). These oscillations lag their respective forcing considerably. Ruddiman and Raymo (2003) devised an age model for the Vostok ice core by tuning the CH<sub>4</sub> signal to low latitude mid-July insolation with no additional lag. Their target curve, which is dominated by precession, effectively lags 21 June 65° N insolation by ~1.6 kyr. They also point out that the CH<sub>4</sub> signal has the same delayed phase as northern ice sheets at the obliquity timescale.

The exact nature of the link between insolation and variations in past atmospheric CH<sub>4</sub> concentration is a much-debated topic (Schmidt et al., 2004). The most common view on CH<sub>4</sub> variations at orbital timescales is that Northern Hemisphere (NH) extratropical (boreal) emissions are mainly influenced by changes in temperature, while tropical emissions are governed by changes in precipitation, i.e. monsoon intensity (Blunier et al., 1995). The land-sea temperature contrast that forces monsoon systems is sensitive to changes in insolation, in particular the 23-kyr cycle which therefore greatly influences the strength of monsoon systems (Kutzbach et al., 2008).

Given that the bulk of emissions originates from the tropical zones with a modest contribution from the extra-tropical NH, and negligible Southern Hemisphere (SH) emission (Walter et al., 2001; Prigent et al., 2007), it seems likely that changes in atmospheric CH<sub>4</sub> concentrations are primarily forced by changes in monsoon intensity (Chappellaz et al., 1990). However, Crowley (1991) noted that past atmospheric CH<sub>4</sub> concentrations

## Methane variations on orbital timescales: a transient modeling experiment

T. Y. M. Konijnendijk et al.

Title Page

Abstract

Introduction

Conclusions

References

Tables

Figures

⏪

⏩

◀

▶

Back

Close

Full Screen / Esc

Printer-friendly Version

Interactive Discussion



compared just as favorably to reconstructed mid-latitude temperatures as they do to simulated Asian monsoon intensity. Therefore, changes in boreal emissions may well be the cause of the observed 23-kyr oscillation in atmospheric CH<sub>4</sub>.

Modeling studies have recently been performed to investigate global wetland area and associated CH<sub>4</sub> emissions during the LGM (Kaplan, 2002; Valdes et al., 2005; Kaplan et al., 2006; Weber et al., 2010), thus implicitly focusing on the effects particular to a glacial termination. Here we perform a 650 000 year transient modeling experiment, with the aim to examine the climatic origin of orbital cycles in atmospheric methane. Focus is on the precession and obliquity (41-kyr) cycles. Questions that we want to address are whether the observed cycles in CH<sub>4</sub> originate in the tropics, in the boreal zone and/or specifically in the Indian/Asian monsoon area; which climatic parameters play an important role in each of these regions; and how we can interpret the lags that have been found in the measured data with respect to the orbital forcing.

Wetland CH<sub>4</sub> emissions over the last 650 000 years are derived from a transient climate simulation with an atmosphere-vegetation-ocean model of intermediate complexity (CLIMBER-2). The climate model output is used to force an off-line model that computes the global distributions of wetland area and CH<sub>4</sub> emissions (TRENCH). Section 2 describes the models used. In Sect. 3 we analyze simulated emissions and examine the relative contribution to emission variations of the tropics, the boreal zone, and the Indian/Asian (I/A) monsoon area. The influence of changes in temperature, vegetation and hydrological processes is analyzed for each of the three regions. In section 4 we discuss the results, compare model output to observational data, and draw conclusions.

## Methane variations on orbital timescales: a transient modeling experiment

T. Y. M. Konijnendijk et al.

Title Page

Abstract

Introduction

Conclusions

References

Tables

Figures



Back

Close

Full Screen / Esc

Printer-friendly Version

Interactive Discussion



## 2 Models and methods

### 2.1 The climate model

As a basis for simulating CH<sub>4</sub> emissions, the CLIMate and BiosphERe model (CLIMBER-2; Petoukhov et al., 2000) was used. This is a coupled atmosphere-ocean-vegetation model of intermediate complexity that is suitable for long simulations due to its fast turnaround time. The model consists of a statistical-dynamical atmosphere, which resolves the large-scale flow that arises due to spatial temperature gradients. It parameterizes atmospheric transports due to synoptic-scale variations in a sophisticated manner (Petoukhov et al., 2000), but it does not contain the weather events themselves. The other components are a 3-basin zonally averaged ocean, including sea ice, and a terrestrial vegetation model VECODE (VEgetation COntinuous DEscription; Brovkin et al., 1997). The latter computes the fraction of the potential vegetation in a grid cell (i.e., grass, trees, and bare soil) as a function of the annual sum of positive day-temperatures and the annual precipitation. The atmospheric model of CLIMBER-2 has a resolution of 10° in latitude and 51.43° in longitude.

With CLIMBER-2 we performed a climate simulation for the interval 650 kyr BP to present, using orbital forcing (Laskar, 2004). Time-varying NH ice sheets and greenhouse gas concentrations (GHG) are prescribed. The volumes of the Laurentide and the Eurasian ice sheet were obtained from a 3-D ice sheet model coupled to a model of deep-ocean temperature (Bintanja et al., 2005). This model was forced by marine benthic oxygen isotopes (Lisiecki and Raymo, 2005) and was run in an inverse mode resulting in timeseries of the Laurentide and Eurasian ice sheet volumes. These volumes were translated into a surface area and height based on the ICE-5G distribution for the LGM until present (Peltier, 2005), set on the spatial grid of CLIMBER-2. Sea level effects due to changes in ice volume are not considered in this study. The increased capacity of continental flats falling dry for wetlands could partially compensate for the loss of boreal wetland area due to ice cover (Weber et al., 2010). However, this

## Methane variations on orbital timescales: a transient modeling experiment

T. Y. M. Konijnendijk et al.

Title Page

Abstract

Introduction

Conclusions

References

Tables

Figures

⏪

⏩

◀

▶

Back

Close

Full Screen / Esc

Printer-friendly Version

Interactive Discussion



effect is difficult to simulate within the CLIMBER-2 grid and it is likely a minor factor in comparison to the main climate factors that are considered in this study.

GHG concentrations (CO<sub>2</sub> and CH<sub>4</sub>) were derived from EPICA Dome C, with the EDC-3 timescale (Lüthi et al., 2008; Loulergue et al., 2008). For the last 500 years we used values from several sources (Robertson et al., 2001). The total greenhouse gas forcing is dominated by CO<sub>2</sub>. Therefore, the simulated climate is only determined by the measured CH<sub>4</sub> concentration variations to a very limited extent. The CLIMBER-2 simulation is described in detail by Weber and Tuenter (2011).

For the present purpose of estimating wetland CH<sub>4</sub> emissions over orbital timescales it is relevant to assess the model's sensitivity to the different forcings involved. These include both internal forcing mechanisms, such as ice sheets and greenhouse gases, as well as external orbital forcing. Compared to General Circulation Models (GCMs), the main drawback of CLIMBER-2 is obviously its coarse resolution and associated parameterizations of small-scale dynamical processes. CLIMBER-2 is however successful in simulating cold climates like the LGM (Ganopolski et al., 1998a), showing a similar sensitivity and response pattern as comprehensive GCMs to the separate impacts of large continental ice sheets and reduced greenhouse gases (Schneider von Deimling et al., 2006). Also, the strength of the NH monsoon during an orbitally forced period like the mid-Holocene lies within the range simulated by GCMs (Ganopolski et al., 1998b; Braconnot et al., 2007). Leads and lags with respect to the orbital forcing were also found to be similar to those found in more complex models (Tuenter et al., 2005; Kutzbach et al., 2008). CLIMBER-2 thus seems capable of adequately representing climatic change in response to different forcings, albeit only at a large spatial scale.

## 2.2 CH<sub>4</sub> emissions model

The wetland and CH<sub>4</sub> emission model TRENCH (TRansient Emissions of Natural CH<sub>4</sub>) is driven off-line by 100-yr averaged monthly output from CLIMBER-2. The monthly output permits the analysis of seasonal variations in wetlands and CH<sub>4</sub> emissions.

### Methane variations on orbital timescales: a transient modeling experiment

T. Y. M. Konijnendijk et al.

Title Page

Abstract

Introduction

Conclusions

References

Tables

Figures

⏪

⏩

◀

▶

Back

Close

Full Screen / Esc

Printer-friendly Version

Interactive Discussion



TRENCH consists of two consecutive components: a wetland extent algorithm and a CH<sub>4</sub> emission algorithm. The wetland location algorithm follows the approach originally proposed by Kaplan (2002), and uses climate variables from CLIMBER-2 that are known to influence wetland formation. Wetland existence is determined based on soil moisture and soil temperature. Wetlands are assumed to exist only during months when the soil temperature is above freezing point. When, in addition, a soil moisture threshold (5% of maximum saturation) is reached, a grid cell is assumed to support wetlands. The fraction of a grid cell covered by wetland is linearly related to the soil moisture value derived from CLIMBER-2 as follows:

$$C_{\text{wet}} = a \times M \times (1 - I) \quad (1)$$

Where  $C_{\text{wet}}$  is the fraction of wetland in a grid cell,  $a$  is a tuning factor,  $M$  is the soil moisture, and  $I$  is the fraction of a grid cell covered with land ice. Resulting grid cell fractions are multiplied with the land surface area in a grid cell to obtain wetland area in km<sup>2</sup>. We assume that orography does not play a role at the present spatial resolution, as a grid cell always contains sufficient flat terrain to support wetlands when climatic conditions allow this. The wetland algorithm was tuned to obtain a reasonable geographical distribution of wetlands and a plausible value for worldwide wetland extent in km<sup>2</sup>, which is comparable to values in literature.

The CH<sub>4</sub> emission algorithm of TRENCH is based on Gedney et al. (2004), who propose a simple model for emissions dependent on wetland fraction, soil carbon content, and temperature. The temperature sensitivity is expressed in the form of a  $Q_{10}$  factor. In the present model we compute time-varying emissions for each grid cell as follows:

$$E = k \times C_{\text{wet}} \times V \times Q_{10}^{T/10} \quad (2)$$

Here  $E$  is the CH<sub>4</sub> emission (in TgCH<sub>4</sub> of a given grid cell at a certain time step and month),  $k$  is a tunable constant,  $C_{\text{wet}}$  is the fraction of wetland in a grid cell as calculated in the wetland distribution model (Eq. 1), and  $V$  a vegetation factor. The temperature sensitivity is expressed in the form of a  $Q_{10}$  factor, with  $T$  the soil temperature in degrees Celsius.

## Methane variations on orbital timescales: a transient modeling experiment

T. Y. M. Konijnendijk et al.

Title Page

Abstract

Introduction

Conclusions

References

Tables

Figures

⏪

⏩

◀

▶

Back

Close

Full Screen / Esc

Printer-friendly Version

Interactive Discussion





## Methane variations on orbital timescales: a transient modeling experiment

T. Y. M. Konijnendijk et al.

Title Page

Abstract

Introduction

Conclusions

References

Tables

Figures

⏪

⏩

◀

▶

Back

Close

Full Screen / Esc

Printer-friendly Version

Interactive Discussion



The  $Q_{10}$  is a temperature-dependant variable itself, because the efficiency of  $\text{CH}_4$  production changes with temperature (Gedney et al., 2004). In literature, values for  $Q_{10}$  vary between 1.7–16 (e.g. Walter and Heimann, 2000). Most studies converge at values around 2–4, but large differences remain as a result of different locations and covarying processes involved when calculating in the  $Q_{10}$  value (Segers, 1998). Studies estimating  $Q_{10}$  values often perform measurements on one or more wetland sites. Because of the global scale of modeling and simplicity of the basic emission model in this study, a range of  $Q_{10}$  values may be plausible. The base value  $Q_{10}(T_0)$  – the  $Q_{10}$  at  $0^\circ\text{C}$  – was set at 2.0, at which value the distribution of  $\text{CH}_4$  emissions over boreal wetlands (north of  $30^\circ\text{N}$ ) and tropical wetlands (latitudes between  $30^\circ\text{N}$  and  $30^\circ\text{S}$ ) agrees with previous observational and modeling studies.

Wetland  $\text{CH}_4$  production also depends on the soil carbon content, which is basically the amount of decomposable organic material in the substrate (Christensen et al., 2003). As this is not simulated by the present version of CLIMBER-2, we used the grass and trees vegetation cover fractions  $F_{\text{grass}}$  and  $F_{\text{trees}}$ , provided by VECODE, as the best estimate. In addition to the production of organic material, vegetation related root systems are important for the transport of  $\text{CH}_4$  to the surface (Rice et al., 2010). Trees have more extensive root systems than grass and the litter that falls of trees provides more organic material than grass. For these reasons we added the two vegetation fractions, attributing 50% more weight to  $F_{\text{trees}}$  than to  $F_{\text{grass}}$ , to form the vegetation factor  $V$ . The results were not found sensitive to the exact percentage value.

The  $k$  factor was chosen to obtain global annual emissions of  $\sim 150\text{ Tg CH}_4$  for the Pre-Industrial Holocene (PIH; 1850 AD). This target value is based on estimates of contemporary wetland emissions by Houweling et al. (2000) and Chen and Prinn (2006). TRENCH was thus tuned to reproduce the basic features of wetland distribution and  $\text{CH}_4$  emissions for the PIH. In order to assess model performance, the results for the LGM were compared to those of earlier studies using GCMs.



## 2.3 Model performance for the PIH and LGM

The calculated maximum global wetland extent for the PIH occurs in June and is  $6.3 \times 10^6 \text{ km}^2$ . During minimum inundation, which occurs in December, the total wetland area is  $3.6 \times 10^6 \text{ km}^2$ . Taking into account that PIH wetlands were possibly  
5  $\sim 20\%$  larger than today due to destruction by agriculture (Chappellaz et al., 1993), this agrees with contemporary estimates based on satellite data of  $5.9 \times 10^6 \text{ km}^2$  and  $2.1 \times 10^6 \text{ km}^2$ , respectively (Prigent et al., 2007). Boreal wetlands (annual average) make out 38% of the global annual mean, which is consistent with estimates for the present (Lehner and Döll, 2004; Prigent et al., 2007). Simulated wetland extent peaks  
10 in high northern latitudes ( $45^\circ \text{ N}$ – $65^\circ \text{ N}$ ), while extensive wetlands are also found in the tropics (Fig. 1).

Total simulated annual emissions amount to 151 Tg  $\text{CH}_4$ , of which 35 Tg (23%) originates in boreal wetlands and 116 Tg (77%) in the tropics. This distribution is in agreement with many previous observational and modeling studies, which find that 15–37%  
15 of the global emissions comes from boreal wetlands and 56–85% originates in tropical wetlands (Cao et al., 1996; Walter et al., 2001; Valdes et al., 2005). Boreal wetland area peaks during early summer when snowmelt rates surge, but the average temperature is still low (Fig. 2). Together with the limited emission season this makes the higher latitudes a less efficient source of  $\text{CH}_4$  than the tropics. Therefore, the peak  
20 in simulated wetland extent in the high latitudes only translates in a moderate level of emissions (Fig. 1).

Global wetland area during the LGM is at its maximum in June with  $5.3 \times 10^6 \text{ km}^2$  and at its minimum in December with  $3.3 \times 10^6 \text{ km}^2$ , a decrease of 17% in the annual-mean compared to the PIH. Boreal wetlands make up  $\sim 26\%$  of the annual global mean,  
25 shifting the main component of wetland extent towards the tropics. This change of distribution is caused by the presence of large continental ice sheets at high latitudes and a relatively dry Eurasian mainland during the LGM due to generally reduced precipitation. There is a decrease in global  $\text{CH}_4$  emissions between the PIH and LGM to

CPD

7, 47–77, 2011

### Methane variations on orbital timescales: a transient modeling experiment

T. Y. M. Konijnendijk et al.

Title Page

Abstract

Introduction

Conclusions

References

Tables

Figures

⏪

⏩

◀

▶

Back

Close

Full Screen / Esc

Printer-friendly Version

Interactive Discussion



118 Tg CH<sub>4</sub>/yr (21%). Tropical emissions are reduced by 12%, while boreal emissions drop by 58%. Previous GCM-based modeling studies have found similar moderate reductions in global emissions of 16–29% (Kaplan, 2002; Valdes et al., 2005; Kaplan et al., 2006) as well as stronger reductions of 29–42% (Weber et al., 2010).

A large cooling occurs in higher latitudes during the LGM. For example, Wu et al. (2007) reconstructed a 10 °C surface cooling in the Northern Hemisphere (NH), while only minor to moderate cooling takes place in the tropics: 0–3 °C. This is accurately simulated by CLIMBER-2 (Fig. 3). The strong cooling of the boreal zone limits the ability of large areas to sustain wetlands during most of the year due to the temperature constraint (Sect. 2.2). This temperature-effect is larger than the direct loss of wetland area by ice cover. Additionally, the decreasing temperature has a negative impact on vegetation growth. Figure 3 shows that vegetation cover was strongly diminished in the LGM with respect to the PIH in boreal latitudes, while there is little change in the tropics.

### 3 Main sources and controls of wetland methane emissions

#### 3.1 Simulated emissions in the transient run

Figure 4 shows timeseries of the forcings used in the transient run, namely ice volume, greenhouse gas variations and insolation at 65° N as an illustration of the orbital forcing. We also show the global mean values of the main climatic parameters, as derived from CLIMBER-2, determining wetland CH<sub>4</sub> emissions, wetland extent and the emission temperature (average temperature over grid cells emitting CH<sub>4</sub>), as well as the vegetation cover. All parameters show variations on multiple (orbital) timescales. Simulated temperature and vegetation changes, together with the varying wetland distribution, were used to compute total annual and global CH<sub>4</sub> emissions. These were found to vary between 116 and 167 Tg/yr. In Fig. 5 the global CH<sub>4</sub> emissions are compared to the atmospheric CH<sub>4</sub> concentrations derived from EDC. The EDC-3 curve

## Methane variations on orbital timescales: a transient modeling experiment

T. Y. M. Konijnendijk et al.

[Title Page](#)[Abstract](#)[Introduction](#)[Conclusions](#)[References](#)[Tables](#)[Figures](#)[⏪](#)[⏩](#)[◀](#)[▶](#)[Back](#)[Close](#)[Full Screen / Esc](#)[Printer-friendly Version](#)[Interactive Discussion](#)

shows pronounced sub-orbital variability, which is absent from the simulated curve. This is because CLIMBER-2 lacks internally-generated variations on these timescales. Simulated climate and vegetation are driven by the applied forcings, which vary on orbital timescales. The longer-timescale variations (>3 kyr) in both curves correspond very well ( $r = 0.79$ ).

As wetlands are the main natural source, wetland CH<sub>4</sub> emissions for a large part determine atmospheric concentrations during this period. Therefore we directly compare measured concentrations and simulated wetland emissions here. Spectra of the two time series were determined using Analyseries (Paillard et al., 1996). Both spectra (Fig. 6) indicate a strong 100 kyr signal and significant influence of 41 kyr oscillations. Precession related features (i.e. 23 kyr) show a stronger signal in the model results than in the measured data. However, differences in the relative importance of spectral peaks in measured concentrations and simulated global emissions could be due to lifetime variations that cannot be accounted for in the present model set-up. The atmospheric CH<sub>4</sub> lifetime was tentatively diagnosed from the measured concentrations and simulated total wetland emissions. Assuming a constant biomass burning source of 40 Tg CH<sub>4</sub>/yr (Fisher et al., 2008) and additional covarying sources, like ruminants, termites and geological sources, amounting to 30 Tg CH<sub>4</sub>/yr during the PIH (Denman et al., 2007), we find that lifetimes vary between ~5.5 year during periods of low CH<sub>4</sub> concentrations, and ~9 year during periods of high CH<sub>4</sub> concentrations. These are reasonable values, which support our conclusion of close correspondence between the measured and simulated timeseries.

In order to further analyze the origin of simulated wetland emissions we separately consider three regions (Fig. 7): the areas influenced by the I/A summer monsoon, the boreal area north of 30° N, but excluding the East Asian monsoon grid box, and the tropical area, 30° S–30° N, excluding the remaining monsoon-dominated grid boxes. The I/A monsoon is analyzed separately as this area is generally assumed to be an important source of wetland emissions (Kutzbach et al., 2008). Moreover, this area is found to exhibit different behavior from the equatorial tropics where shifts in the

## Methane variations on orbital timescales: a transient modeling experiment

T. Y. M. Konijnendijk et al.

Title Page

Abstract

Introduction

Conclusions

References

Tables

Figures

⏪

⏩

◀

▶

Back

Close

Full Screen / Esc

Printer-friendly Version

Interactive Discussion



Intertropical Convergence Zone (ITCZ) determine whether wetlands can exist or not. The bulk of global emissions (72% during the PIH) are emitted from the tropics. The boreal zone and the monsoon areas contribute the remainder (18% and 9% respectively). The spectra for the individual regions (Fig. 6) show that they each have a typical timescale behavior, as mentioned above. Emissions from the I/A monsoon area are primarily controlled by precession, with little to no influence from 100 kyr and 41 kyr. Boreal emissions mainly reflect 41 kyr and 100 kyr signals, while tropical emissions contain a strong precession signal and significant power at the 41 kyr and 100 kyr frequencies.

The EDC-3 record for CH<sub>4</sub> and the time series for simulated global emissions, as well as those of the separate regions, were band pass filtered using Analyseries (Pailliard et al., 1996) at 21 ( $\pm 2.5$ ) kyr and 41 ( $\pm 3.5$ ) kyr. The filtered signals were then cross correlated to the astronomical precession index and obliquity parameter, respectively (Laskar, 2004). The measured EDC-3 derived methane concentration is found to lag the orbital forcing by 2.0 kyr on the precession timescale and by 5.5 kyr on the obliquity timescale (Table 1). For the simulated global emissions lags are 1.3 kyr and 5.3 kyr, respectively, (Fig. 8). We consider this a very close match given that climate models are generally not successful in reproducing lags found in measured data (e.g. Ziegler et al., 2010). Lags are longest for emissions from the boreal zone and smallest for emissions from the monsoon areas, with intermediate lags for tropical emissions (Table 1).

### 3.2 Factor analyses

The next step is to analyze the climate and vegetation factors that control variations in simulated CH<sub>4</sub> emissions and the simulated lags. First we define a total modification factor  $F_{\text{tot}}$  as follows:

$$F_{\text{tot}}(t) = E(t)/E_{\text{PIH}} \quad (3)$$

where  $E$  denotes annual emissions,  $t$  is time and  $E_{\text{PIH}}$  denotes annual emissions during the PIH. According to Eq. (2) there are three individual factors determining the total

CPD

7, 47–77, 2011

## Methane variations on orbital timescales: a transient modeling experiment

T. Y. M. Konijnendijk et al.

Title Page

Abstract

Introduction

Conclusions

References

Tables

Figures

⏪

⏩

◀

▶

Back

Close

Full Screen / Esc

Printer-friendly Version

Interactive Discussion



emission changes, namely changes in wetland cover ( $F_c$ ), in vegetation cover ( $F_v$ ) and in temperature ( $F_t$ ). To compute individual modification factors for each grid box, one term in Eq. (2) was set at its transient value and the other two terms were set at PIH values. The results were then divided by the emissions of that grid box for the PIH.

5 Equation (5) shows this factorial calculation for wetland cover ( $F_c$ ):

$$F_c(t) = k \times C(t) \times V_{\text{PIH}} \times Q_{10, \text{PIE}}^{T/10} / E_{\text{PIH}} \quad (4)$$

where  $k$  is the unaltered tunable constant,  $C(t)$  is the transient wetland cover,  $V_{\text{PIH}}$  is the vegetation cover and  $Q_{10, \text{PIH}}^{T/10}$  is the temperature dependence, both fixed at their PIH values. For each grid box  $F_{\text{tot}}$  is equal to  $F_c \times F_v \times F_t$ . The results from the factor analysis are averaged globally and for the three separate zones defined above using a weighted average. By weighing the modification factors of each grid box according to their PIH emissions in the averaging process, skewing effects of extreme modifications in low-emission cells such as in high boreal latitudes are countered.

15 Timeseries of the modification factors (Fig. 9) show that temperature is the dominant control both for tropical and boreal emissions, with vegetation as a secondary role. During cold periods wetland extent is a reducing factor in the boreal zone, but an amplifying factor in the tropics, possibly related to reduced evaporation. However, the effect is small in both zones and almost cancels out in the global mean. Wetlands coverage is only an important factor in the I/A monsoon region, together with vegetation changes.

20 Spectral analyses (Fig. 10) show that precession-related variability is dominated by vegetation changes in the tropics and in the I/A monsoon region, while in the boreal zone a combination of temperature and vegetation changes play a role. This results in global emissions dominated by vegetation at the precession timescale, with a smaller impact from temperature. At the obliquity timescale temperature and vegetation are equally important in global emissions, which reflect both boreal and tropical results. Vegetation only dominates in the I/A monsoon area. The 100-kyr variations in global emissions are primarily determined by temperature, which is a global phenomena

## Methane variations on orbital timescales: a transient modeling experiment

T. Y. M. Konijnendijk et al.

Title Page

Abstract

Introduction

Conclusions

References

Tables

Figures

⏪

⏩

◀

▶

Back

Close

Full Screen / Esc

Printer-friendly Version

Interactive Discussion



present in all three zones.

To summarize, at the precession timescale vegetation is the dominant control of global methane emissions, with temperature as a secondary control. The dominance of vegetation control originates primarily from the tropics. There is also a clear impact of vegetation in the I/A monsoon area, but these constitute only a small part of the global emissions. At the obliquity timescale temperature and vegetation play equally important roles. The temperature changes are almost completely in phase with ice volume minima/greenhouse gas maxima. Vegetation changes lag summer insolation maxima by ca. 1kyr for precession to 2–4kyr for obliquity (Table 1). This reflects the strong influence of hydrological processes, which respond quasi-instantaneously to the orbital forcing, on vegetation. For both temperature and vegetation lags tend to be longer in the boreal zone than in the tropics (Table 1). The combined effect of temperature and vegetation, explains the lags that are found between simulated methane emissions and the orbital forcings.

#### 4 Summary, discussion and conclusions

We have simulated wetland CH<sub>4</sub> emissions over the last 650 000 yrs using a simple wetland distribution and CH<sub>4</sub> emissions model coupled off-line to the atmosphere-ocean-vegetation climate model CLIMBER-2. The resulting simulated global emissions show a close similarity to the measured EDC-3 timeseries of atmospheric CH<sub>4</sub> concentrations, both in spectra and in lags with respect to the orbital forcing. Diagnosed CH<sub>4</sub> lifetimes vary between ~5.5 and 9 yr on glacial-interglacial timescales, with 8.2 yrs as estimated for the PIH. This is consistent with data (Fisher et al., 2008) and model studies that include atmospheric chemistry (Lelieveld et al., 1998).

Global emissions are dominated by emissions from the tropics. However, in contrast to the general assertion that monsoon intensity is of primary importance (Chappellaz et al., 1990; Blunier et al., 1995) we find that temperature and vegetation changes are the main drivers. The I/A monsoon area is too small in size to contribute substantially

## Methane variations on orbital timescales: a transient modeling experiment

T. Y. M. Konijnendijk et al.

Title Page

Abstract

Introduction

Conclusions

References

Tables

Figures

⏪

⏩

◀

▶

Back

Close

Full Screen / Esc

Printer-friendly Version

Interactive Discussion



## Methane variations on orbital timescales: a transient modeling experiment

T. Y. M. Konijnendijk et al.

Title Page

Abstract

Introduction

Conclusions

References

Tables

Figures

⏪

⏩

◀

▶

Back

Close

Full Screen / Esc

Printer-friendly Version

Interactive Discussion

to global emissions. As hypothesized by Crowley (1999), monsoon precipitation and global emissions do co-vary, but there is no causal link. For the remainder of the tropics, wetland extent exerts little control on emissions. Tropical temperature variations are found to be small, about 2–4 °C on glacial-interglacial timescales in agreement with proxy data (Farrera et al., 1999). However, such variations are significant as methanogenesis is much more sensitive to temperature changes at the high average temperatures in the tropics than at the lower average temperatures at high latitudes (compare Eq. 2).

The present results show that temperature and vegetation are the dominant controls of orbital-scale variations in global wetland CH<sub>4</sub> emissions, while wetland extent plays a minor role. This is supported by a recent modeling study, based on an eight-member ensemble of GCM simulations for the LGM, which also found temperature and vegetation as the main controlling factors (Weber et al., 2010). In the latter study wetlands exhibited southward shifts in the cold LGM climate, related to a southward shift of the mid-latitude storm tracks and the ITCZ. This caused the effect of changes in wetland distribution to cancel out in the global mean. Here we find a shift from the boreal to the tropical zone. This larger-scale pattern is likely related to the coarse resolution of CLIMBER-2 and the fact that the atmospheric dynamics are simplified, so that storm tracks are not resolved. This is a shortcoming of the present simulation. However, it does not seem to affect our main conclusion on the primary role of temperature and vegetation.

Orbital cycles in vegetation have been found in many studies based on pollen data, for example for tropical South America (Hooghiemstra et al., 1993), Southeast Asia (Tsukada, 1996), Europe (Tzedakis et al., 2009) and North America (Whitlock and Bartlein, 1997). These studies indicate large shifts in vegetation presence and cover type. The vegetation model used in the present study only very crudely resolves such shifts. Nevertheless, we believe that our results on the role of vegetation are qualitatively valid although precise quantitative estimates are not possible using CLIMBER-2.



## Methane variations on orbital timescales: a transient modeling experiment

T. Y. M. Konijnendijk et al.

Title Page

Abstract

Introduction

Conclusions

References

Tables

Figures

⏪

⏩

◀

▶

Back

Close

Full Screen / Esc

Printer-friendly Version

Interactive Discussion

Finally, our results provide a plausible explanation for the lags found in the measured EDC-3 curve with respect to the orbital forcing. Atmospheric CH<sub>4</sub> concentrations have previously been related to monsoon precipitation (Ruddiman and Raymo, 2003). Here we find that lags in the CH<sub>4</sub> record are very likely due to temperature and vegetation effects rather than monsoon precipitation. The former two factors have a phasing in-between insolation maxima and ice sheet/greenhouse gas minima. This results in lags that are very close to those found in measured CH<sub>4</sub> data, both at the precession and obliquity timescale. In contrast, simulated monsoon precipitation has zero lag at the precession band (Weber and Tuenter, 2011). This is inconsistent with any proxy-based estimate, as proxy records which have been interpreted as reflecting Indian/Asian summer monsoons have been found to lag precession by lags varying from 3 kyr (Wang et al., 2008) to considerably longer lags of up to 8 kyr (Clemens and Prell, 2003). Process-based modeling of proxies seems a necessary step to substantiate a reinterpretation of proxy records (Ziegler et al., 2010; Clemens et al., 2010) and to resolve this mismatch among different proxy data as well as between simulated and measured records.

## References

- Bintanja, R., van de Wal, R. S. W., and Oerlemans, J.: Modelled atmospheric temperatures and global sea levels over the past million years, *Nature*, 437, 125–128, 2005.
- Blunier, T., Chappellaz, J., Schwander, J., Stauffer, B., and Raynaud, D.: Variations in atmospheric methane concentration during the Holocene epoch, *Nature*, 374, 46–49, 1995.
- Braconnot, P., Otto-Bliesner, B., Harrison, S., Jousaume, S., Peterchmitt, J.-Y., Abe-Ouchi, A., Crucifix, M., Driesschaert, E., Fichet, Th., Hewitt, C. D., Kageyama, M., Kitoh, A., Lâiné, A., Loutre, M.-F., Marti, O., Merkel, U., Ramstein, G., Valdes, P., Weber, S. L., Yu, Y., and Zhao, Y.: Results of PMIP2 coupled simulations of the Mid-Holocene and Last Glacial Maximum - Part 1: experiments and large-scale features, *Clim. Past*, 3, 261–277, doi:10.5194/cp-3-261-2007, 2007.
- Brovkin, V., Ganopolski, A., and Svirezhev, Y.: A continuous climate-vegetation classification for use in climate-biosphere studies, *Ecol. Model.*, 101, 251–261, 1997.

---

## Methane variations on orbital timescales: a transient modeling experiment

T. Y. M. Konijnendijk et al.

---

[Title Page](#)[Abstract](#)[Introduction](#)[Conclusions](#)[References](#)[Tables](#)[Figures](#)[⏪](#)[⏩](#)[◀](#)[▶](#)[Back](#)[Close](#)[Full Screen / Esc](#)[Printer-friendly Version](#)[Interactive Discussion](#)

- Cao, M., Marshall, S., and Gregson, K.: Global carbon exchange and methane emissions from natural wetlands: Application of a process-based model, *J. Geophys. Res.*, 101, 14399–14414, 1996.
- Chappellaz, J., Barnola, J. M., Raynaud, D., Korotkevich, Y. S., and Lorius, C.: Ice-core record of atmospheric methane over the past 160,000 years, *Nature*, 345, 127–131, 1990.
- Chappellaz, J. A., Fung, I. Y., and Thompson, A.M., The atmospheric CH<sub>4</sub> increase since the Last Glacial Maximum, 1. Source estimates, *Tellus B*, 45, 228–241, 1993.
- Chen, Y. and Prinn, R. G.: Estimation of atmospheric methane emissions between 1996 and 2001 using a three-dimensional global chemical transport model, *J. Geophys. Res.*, 111, D10307, doi:10.1029/2005JD006058, 2006.
- Christensen, T. R., Ekberg, A., Strom, L., Mastepanov, M., Panikov, N., Oquist, M., Svensson, B. H., Nykanen, H., Martikainen, P. J., and Oskarsson, H.: Factors controlling large scale variations in methane emissions from wetlands, *Geophys. Res. Lett.*, 30(7), 1414, doi:2003GL016848, 2003.
- Clemens, S. C., Prell, W. L., and Sun, Y.: Orbital-scale timing and mechanisms driving Late Pleistocene Indo-Asian summer monsoons: reinterpreting cave speleotherm  $\delta^{18}\text{O}$ , *Paleoceanography*, 25, PA4207, doi:10.1029/2010PA001926, 2010.
- Crowley, T. J.: Ice-age methane variations, *Nature*, 353, 122–123, 1991.
- Denman, K. L., Brasseur, G., Chidthaisong, A., Ciais, P., Cox, P. M., Dickinson, R. E., Hauglustaine, D., Heinze, C., Holland, E., Jacob, D., Lohmann, U., Ramachandran, S., da Silva Dias, P. L., Wofsy, S. C., and Zhang, X.: Couplings Between Changes in the Climate System and Biogeochemistry. In: *Climate Change 2007: The Physical Science Basis. Contribution of Working Group I to the Fourth Assessment Report of the Intergovernmental Panel on Climate Change*, edited by: Solomon, S., Qin, D., Manning, M., Chen, Z., Marquis, M., Averyt, K. B., Tignor, M., and Miller, H. L., Cambridge University Press, Cambridge, UK and New York, NY, USA, 2007.
- Fischer, H., Behrens, M., Bock, M., Richter, U., Schmitt, J., Loulergue, L., Chappellaz, J., Spahni, R., Blunier, T., Leuenberger, M., and Stocker, T. F.: Changing boreal methane sources and constant biomass burning during the last termination, *Nature*, 452, 864–867, 2008.
- Fung, I., John, J., Lerner, J., Matthews, E., Prather, M., Steele, L., and Fraser, P.: Three Dimensional Model Synthesis of the Global Methane Cycle, *J. Geophys. Res.* 96, 13033–13065, 1991.

---

## Methane variations on orbital timescales: a transient modeling experiment

T. Y. M. Konijnendijk et al.

---

[Title Page](#)[Abstract](#)[Introduction](#)[Conclusions](#)[References](#)[Tables](#)[Figures](#)[⏪](#)[⏩](#)[◀](#)[▶](#)[Back](#)[Close](#)[Full Screen / Esc](#)[Printer-friendly Version](#)[Interactive Discussion](#)

- Gedney, N., Cox, P. M., and Huntingford, C.: Climate feedback from wetland methane emissions, *Geophys. Res. Lett.*, 31, L20503, doi:10.1029/2004GL020919, 2004.
- Hooghiemstra, H., Melice, J. L., Berger, A., and Shackleton, N. J.: Frequency spectra and paleoclimatic variability of the high-resolution 30–1450 ka Funza I pollen record (Eastern Cordillera, Colombia), *Quaternary Sci. Rev.*, 12(2), 141–156, 1993.
- 5 Houweling, S., Dentener, F., and Lelieveld, J.: Simulation of preindustrial atmospheric methane to constrain the global source strength of natural wetlands, *J. Geophys. Res.*, 105, 243–255, 2000.
- Kaplan, J. O.: Wetlands at the Last Glacial Maximum: Distribution and methane emissions, *Geophys. Res. Lett.*, 29, 6, 2002.
- 10 Kaplan, J. O., Folberth, G., and Hauglustaine, D. A.: Role of methane and biogenic volatile organic compound sources in late glacial and Holocene fluctuations of atmospheric methane concentrations, *Global Biogeochem. Cy.*, 20, 16, 2006.
- Kutzbach, J. E., Liu, X., Liu, Z., and Chen, G.: Simulation of the evolutionary response of global summer monsoons to orbital forcing over the past 280,000 years, *Clim. Dynam.* 30(6), 567–579, 2008.
- 15 Laskar, J., Robutel, P., Joutel, F., Gastineau, M., Correia, A. C. M., and Levrard, B.: A long-term numerical solution for the insolation quantities of the Earth, *Astron. Astrophys.*, 428, 261–285, 2004.
- 20 Lelieveld, J., Crutzen, P., and Dentener, F. J.: Changing concentration, lifetime and climate forcing of atmospheric methane, *Tellus B*, 50, 128–150, 1998.
- Lisiecki, L. and Raymo, M.: A Pliocene-Pleistocene stack of 57 globally distributed benthic  $\delta^{18}\text{O}$  records, *Paleoceanography*, 20, PA1003, doi:10.1029/2004PA001071, 2005.
- Loulergue, L., Parrenin, F., Blunier, T., Barnola, J.-M., Spahni, R., Schilt, A., Raisbeck, G., and Chappellaz, J.: Orbital and millennial-scale features of atmospheric  $\text{CH}_4$  over the past 25 800,000 years, *Nature*, 453, 383–386, 2008.
- Lüthi, D., Floch, M. L., Bereiter, B., Blunier, T., Barnola, J. M., Siegenthaler, U., Raynaud, D., Jouzel, J., Fischer, H., Kawamura, K., and Stocker, T. F.: High-resolution carbon dioxide concentration record 650 000–800 000 years before present, *Nature*, 453, 379–382, 2008.
- 30 Peltier, W. R.: Global glacial isostasy and the surface of the ice-age Earth: The ICE-5G (VM2) model and GRACE, *Annu. Rev. Earth Pl. Sc.*, 32, 111–149, 2004.
- Petoukhov, V., Ganopolski, A., Brovkin, V., Claussen, M., Eliseev, A., Kubatzki, C., and Rahmstorf, S.: CLIMBER-2: a climate system model of intermediate complexity, Part I: model

## Methane variations on orbital timescales: a transient modeling experiment

T. Y. M. Konijnendijk et al.

Title Page

Abstract

Introduction

Conclusions

References

Tables

Figures

⏪

⏩

◀

▶

Back

Close

Full Screen / Esc

Printer-friendly Version

Interactive Discussion



- description and performance for present climate, *Clim. Dynam.*, 16, 1–17, 2000.
- Prigent, C., Papa, F., Aires, F., Rossow, W. B., and Matthews, E.: Global inundation dynamics inferred from multiple satellite observations, 1993–2000, *J. Geophys. Res.*, 112, D12107, doi:10.1029/2006JD007847, 2007.
- 5 Rice, A. L., Butenhoff, C. L., Shearer, M. J., Teama, D., Rosenstiel, T. N., and Khalil, M. A. K.: Emissions of anaerobically produced methane by trees, *Geophys. Res. Lett.*, 37, L03807, doi:10.1029/2009GL041565, 2010.
- Ruddiman, W. F. and Raymo, M. E.: A methane-based time scale for Vostok ice, *Quaternary Sci. Rev.*, 22, 141–155, 2003.
- 10 Schmidt, G. A., Shindell, D. T., and Harder, S.: A note on the relationship between ice core methane concentrations and insolation, *Geophys. Res. Lett.*, 31, L23206, doi:10.1029/2004GL021083, 2004.
- Schneider von Deimling, T., Held, H., Ganopolski, A., and Rahmstorf, S.: Climate sensitivity estimated from ensemble simulations of glacial climate, *Clim. Dynam.*, 27, 149–163, 2006.
- 15 Segers, R.: Methane production and methane consumption: a review of processes underlying wetland methane fluxes, *Biogeochemistry*, 41, 23–51, 1998.
- Spahni, R., Chappellaz, J., Stocker, T. F., Loulergue, L., Hausammann, G., Kawamura, K., Fickiger, J., Schwander, J., Raynaud, D., Masson-Delmotte, V., and Jouzel, J.: Atmospheric Methane and Nitrous Oxide of the Late Pleistocene from Antarctic Ice Cores, *Science*, 310, 1317–1321, 2005.
- 20 Tsukada, M.: Late Pleistocene vegetation and climate in Taiwan (Formosa), *P. Natl. Acad. Sci.*, 55, 543–548, 1966.
- Tzedakis, P. C., Palike, H., Roucoux, K. H., and de Abreu, L.: Atmospheric methane, southern European vegetation and low-mid latitude links on orbital and millennial timescales, *Earth Planet. Sc. Lett.*, 277(3–4), 307–317, 2009
- 25 Valdes, P. J., Beerling, D. J., and Johnson, C. E.: The ice age methane budget, *Geophys. Res. Lett.*, 32, L02704, doi:10.1029/2004GL021004, 2005.
- Walter, B. P., Heimann, M., and Matthews, E.: Modeling modern methane emissions from natural wetlands: 1. Model description and results, *J. Geophys. Res.*, 106, 189–234, 2001.
- 30 Wang, W.-C., Yung, Y. L., Lacis, A. A., Mo, T., and Hansen, J. E.: Greenhouse effects due to man-made perturbations of trace gases, *Science*, 194, 685–690, 1996.
- Wang, Y., Cheng, H., Edwards, R. L., Kong, X., Shao, X., Chen, S., Wu, J., Jiang, X., Wang, X., and An, Z.: Millennial- and orbital-scale changes in the East Asian monsoon over the past

## Methane variations on orbital timescales: a transient modeling experiment

T. Y. M. Konijnendijk et al.

Title Page

Abstract

Introduction

Conclusions

References

Tables

Figures

⏪

⏩

◀

▶

Back

Close

Full Screen / Esc

Printer-friendly Version

Interactive Discussion



224,000 years, *Nature*, 451, 1090–1093, 2008.

Weber, S. L., Drury, A. J., Toonen, W. H. J., and van Weele, M.: Wetland methane emissions during the Last Glacial Maximum estimated from PMIP2 simulations: Climate, vegetation, and geographic controls, *J. Geophys. Res.*, 115, DO6111, doi: 10.1029/2009JD012110, 2010.

Weber, S. L. and Tüenter, E.: The impact of varying ice sheets and greenhouse gases on the intensity and timing of boreal summer monsoons, *Quaternary Sci. Rev.*, in press, 2010.

Whitlock, C. and Bartlein, P. J.: Vegetation and climate change in northwest America during the past 125 kyr, *Nature*, 388, 57–61, 1997.

Wu, H., Guiot, J., Brewer, S., and Guo, Z.: Climatic changes in Eurasia and Africa at the Last Glacial Maximum and mid-Holocene: Reconstruction from pollen data using inverse vegetation modeling, *Clim. Dynam.*, 29, 211–229, 2007.

Ziegler, M., Lourens, L. J., Tüenter, E., Hilgen, F., Reichert, G.-J., and Weber, S. L.: Precession phasing offset between Indian summer monsoon and Arabian Sea productivity linked to changes in Atlantic overturning circulation, *Paleoceanography*, 25, PA3213, doi:10.1029/2009PA001884, 2010.

## Methane variations on orbital timescales: a transient modeling experiment

T. Y. M. Konijnendijk et al.

**Table 1.** Lags with respect to the orbital forcing in ice cover, greenhouse gases and EDC-3 atmospheric CH<sub>4</sub>, in the TRENCH simulated global and regional emissions and in the global modification factors. Lags are computed by searching for the optimum correlation between the forcing (precession or obliquity) and a given variable, band pass filtered at 21 kyr or 41 kyr, respectively. Zero phase is set at minimum precession and maximum obliquity, which each correspond to an insolation maximum for the NH. The correlation value is displayed next to the lag.

factor	precession	Correlation	obliquity	Correlation
Ice cover	4.7	−0.86	7.1	−0.94
GHG	–	–	6.0	0.91
EDC-3	2.0	0.78	5.5	0.95
global emissions	1.3	0.93	5.3	0.96
boreal emissions	2.5	0.88	6.3	0.97
tropical emissions	0.7	0.95	4.4	0.96
Indian/Asian monsoon emissions	0.5	0.95	2.6	0.96
Global modification factor	1.1	0.94	4.7	0.97
Global wetland modification factor	2.1	0.88	3.2	0.95
Global vegetation modification factor	0.5	0.94	3.2	0.97
Global temperature modification factor	2.1	0.87	6.9	0.96

[Title Page](#)
[Abstract](#)
[Introduction](#)
[Conclusions](#)
[References](#)
[Tables](#)
[Figures](#)




[Back](#)
[Close](#)
[Full Screen / Esc](#)
[Printer-friendly Version](#)
[Interactive Discussion](#)


## Methane variations on orbital timescales: a transient modeling experiment

T. Y. M. Konijnendijk et al.

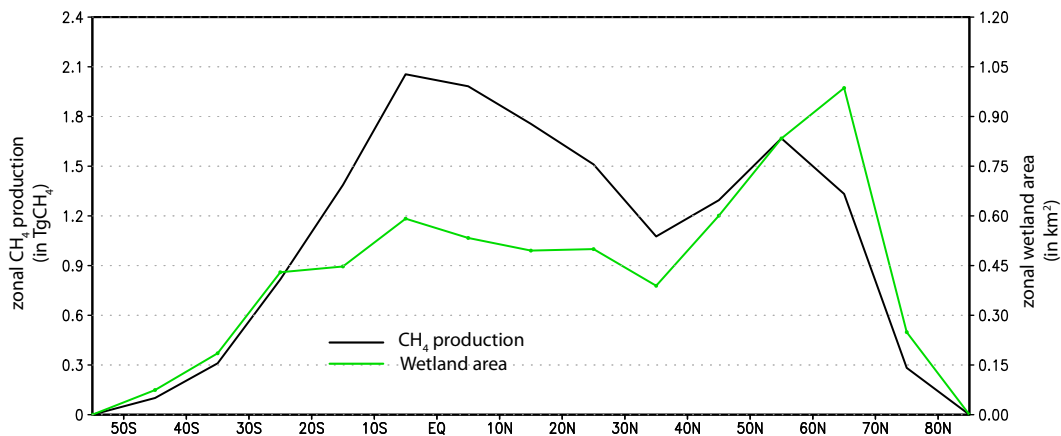


**Fig. 1.** TRENCH simulated PIH wetlands during the month of maximum wetland extent (green line), and emissions (black line), both integrated zonally and by 10° latitude belts.

[Title Page](#)[Abstract](#)[Introduction](#)[Conclusions](#)[References](#)[Tables](#)[Figures](#)[⏪](#)[⏩](#)[◀](#)[▶](#)[Back](#)[Close](#)[Full Screen / Esc](#)[Printer-friendly Version](#)[Interactive Discussion](#)



## Methane variations on orbital timescales: a transient modeling experiment

T. Y. M. Konijnendijk et al.

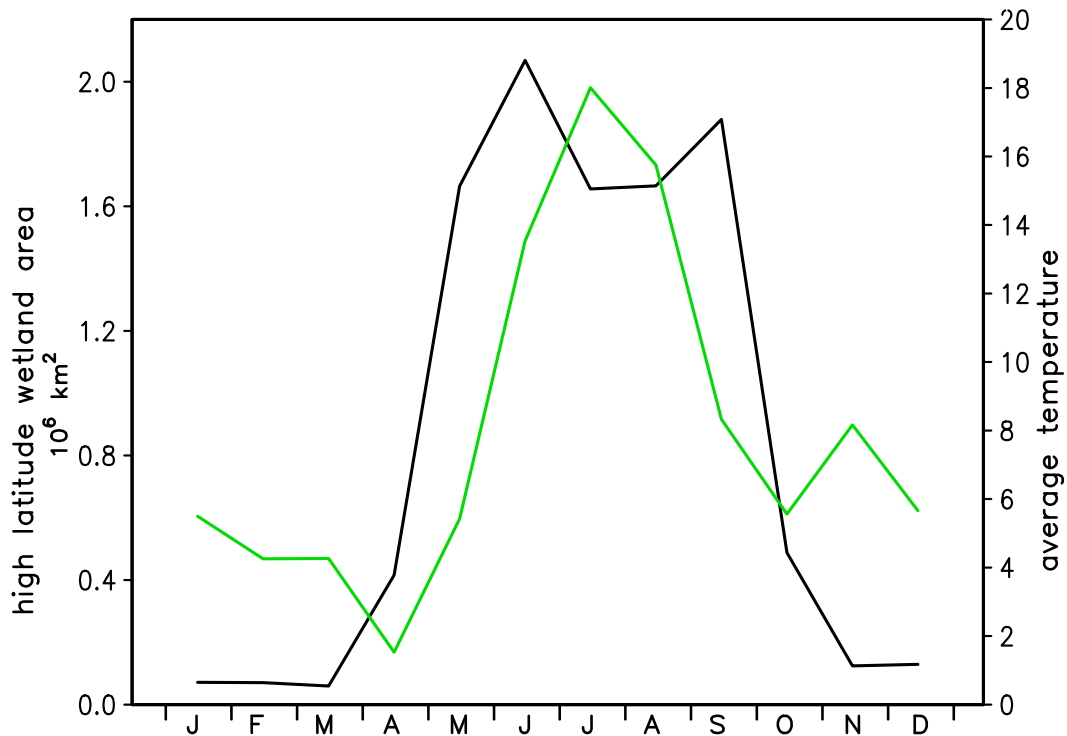


**Fig. 2.** Seasonal variation of high (55–75° N) latitude boreal wetland extent (black line) and soil temperature (green line) during the PIH.

Title Page

Abstract

Introduction

Conclusions

References

Tables

Figures

◀

▶

◀

▶

Back

Close

Full Screen / Esc

Printer-friendly Version

Interactive Discussion

## Methane variations on orbital timescales: a transient modeling experiment

T. Y. M. Konijnendijk et al.

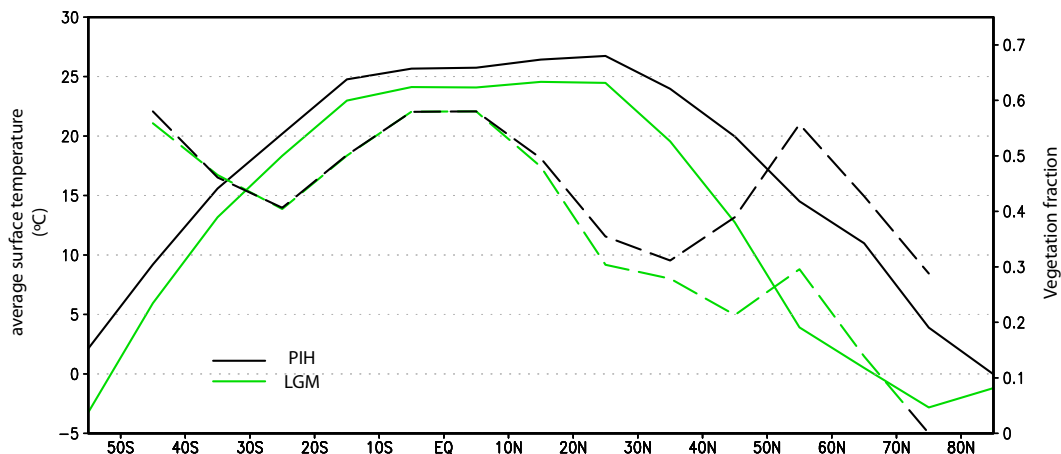


**Fig. 3.** CLIMBER-2 simulated PIH temperature (solid black line) and LGM temperature (solid green line) for the NH summer months, and annual-mean grid-box vegetation factor (Sect. 2.2) during the PIH (dashed black line) and LGM (dashed green line). All data are integrated zonally and by 10° latitude belts.

Title Page

Abstract

Introduction

Conclusions

References

Tables

Figures

◀

▶

◀

▶

Back

Close

Full Screen / Esc

Printer-friendly Version

Interactive Discussion

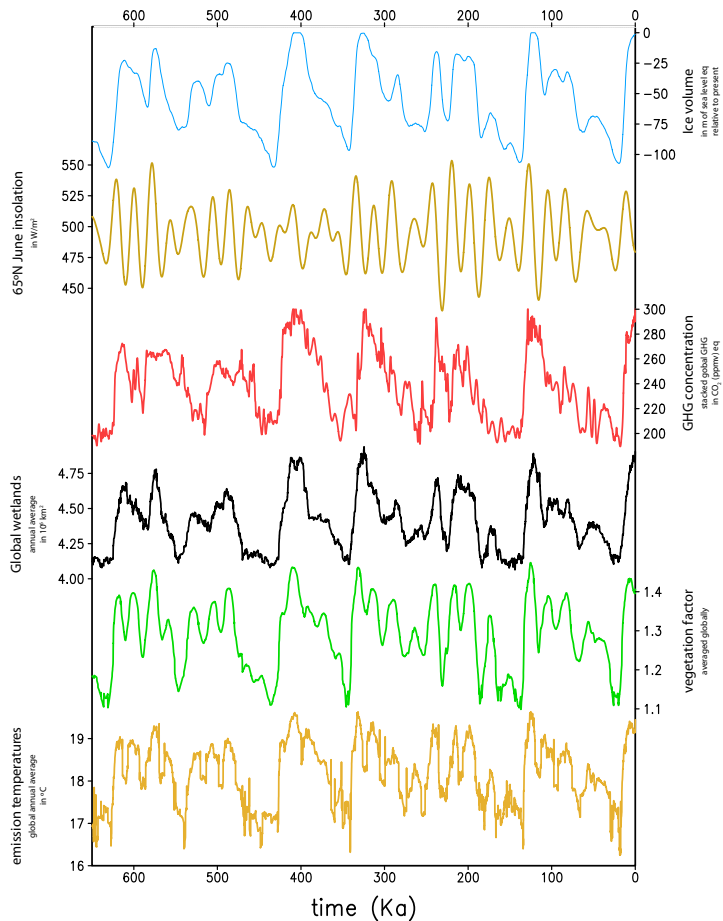


**Fig. 4.** Transient forcings (top graphs) for CLIMBER-2 and the resulting wetland extent, vegetation factor and mean emission temperature (lower graphs).

## Methane variations on orbital timescales: a transient modeling experiment

T. Y. M. Konijnendijk et al.

Title Page

Abstract	Introduction
Conclusions	References
Tables	Figures

⏪      ⏩  
⏴      ⏵

Back      Close

Full Screen / Esc

Printer-friendly Version

Interactive Discussion



## Methane variations on orbital timescales: a transient modeling experiment

T. Y. M. Konijnendijk et al.

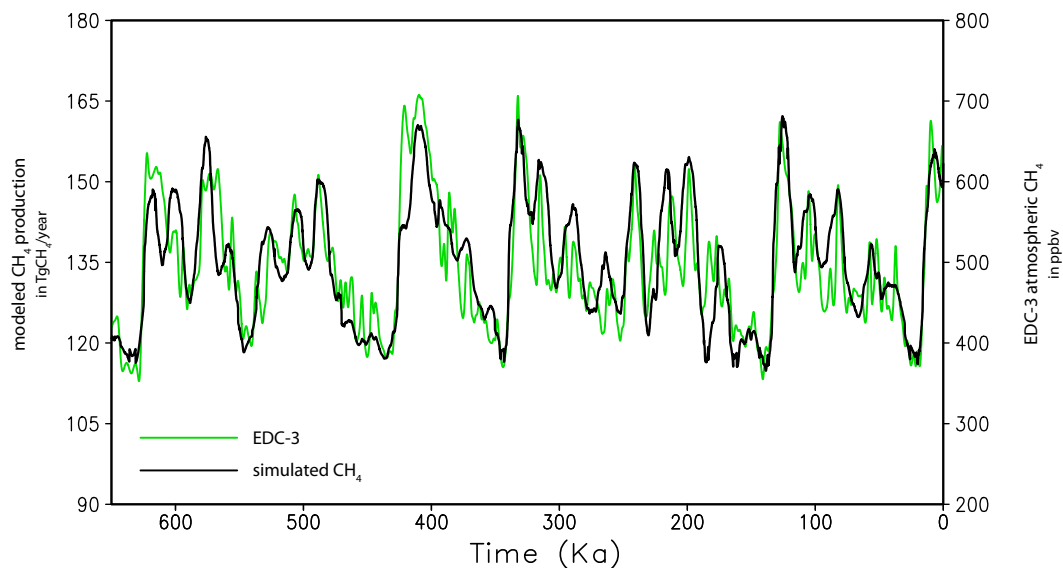


**Fig. 5.** Epica Dome C atmospheric CH<sub>4</sub> concentrations (green line; in ppbv), low pass filtered for timescales longer than 3 kyr, and TRENCH simulated annual global CH<sub>4</sub> emissions (black line; in TgCH<sub>4</sub>).

[Title Page](#)[Abstract](#)[Introduction](#)[Conclusions](#)[References](#)[Tables](#)[Figures](#)[⏪](#)[⏩](#)[◀](#)[▶](#)[Back](#)[Close](#)[Full Screen / Esc](#)[Printer-friendly Version](#)[Interactive Discussion](#)

## Methane variations on orbital timescales: a transient modeling experiment

T. Y. M. Konijnendijk et al.

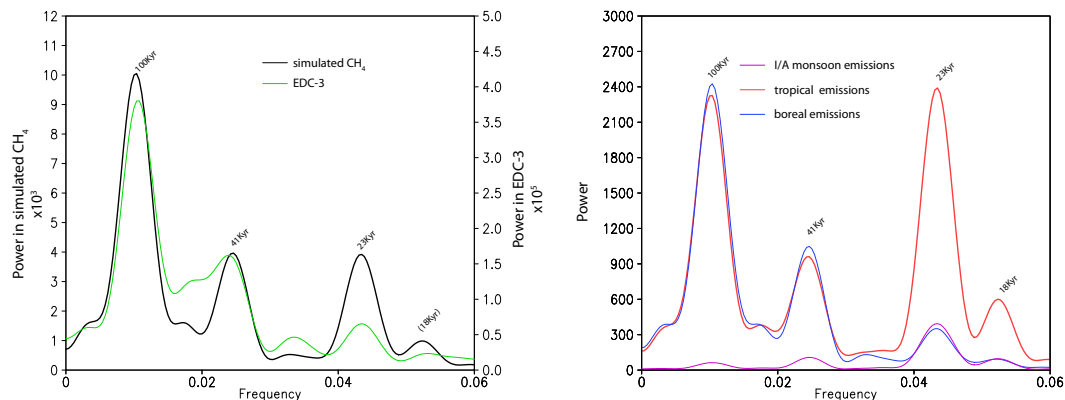


**Fig. 6.** Left: Spectra for the Epica Dome C atmospheric CH<sub>4</sub> concentrations (green line) and the TRENCH simulated annual global CH<sub>4</sub> emissions (black line), both computed over the time series extending from 650 kyr to 0 kyr BP. (right). Spectra for the time series of the separate emissions from the tropical zone (red line), the boreal zone (blue line) and the I/A monsoon areas (violet line); the areas are depicted in Fig. 7.

Title Page

Abstract

Introduction

Conclusions

References

Tables

Figures

⏪

⏩

◀

▶

Back

Close

Full Screen / Esc

Printer-friendly Version

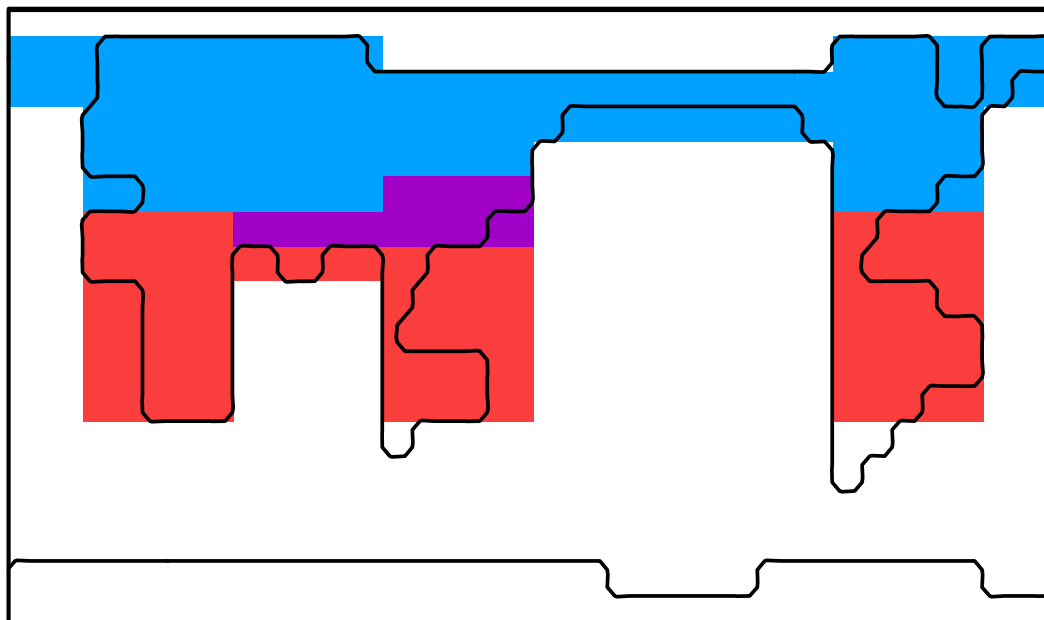
Interactive Discussion




---

## Methane variations on orbital timescales: a transient modeling experiment

T. Y. M. Konijnendijk et al.

---

[Title Page](#)[Abstract](#)[Introduction](#)[Conclusions](#)[References](#)[Tables](#)[Figures](#)[⏪](#)[⏩](#)[◀](#)[▶](#)[Back](#)[Close](#)[Full Screen / Esc](#)[Printer-friendly Version](#)[Interactive Discussion](#)

-  tropical zone
-  boreal zone
-  Indian/Asian monsoon areas

**Fig. 7.** Definition of the tropical (red), boreal (blue) and Indian/Asian monsoon (pink) zones. Emissions from these three zones are separately analyzed.

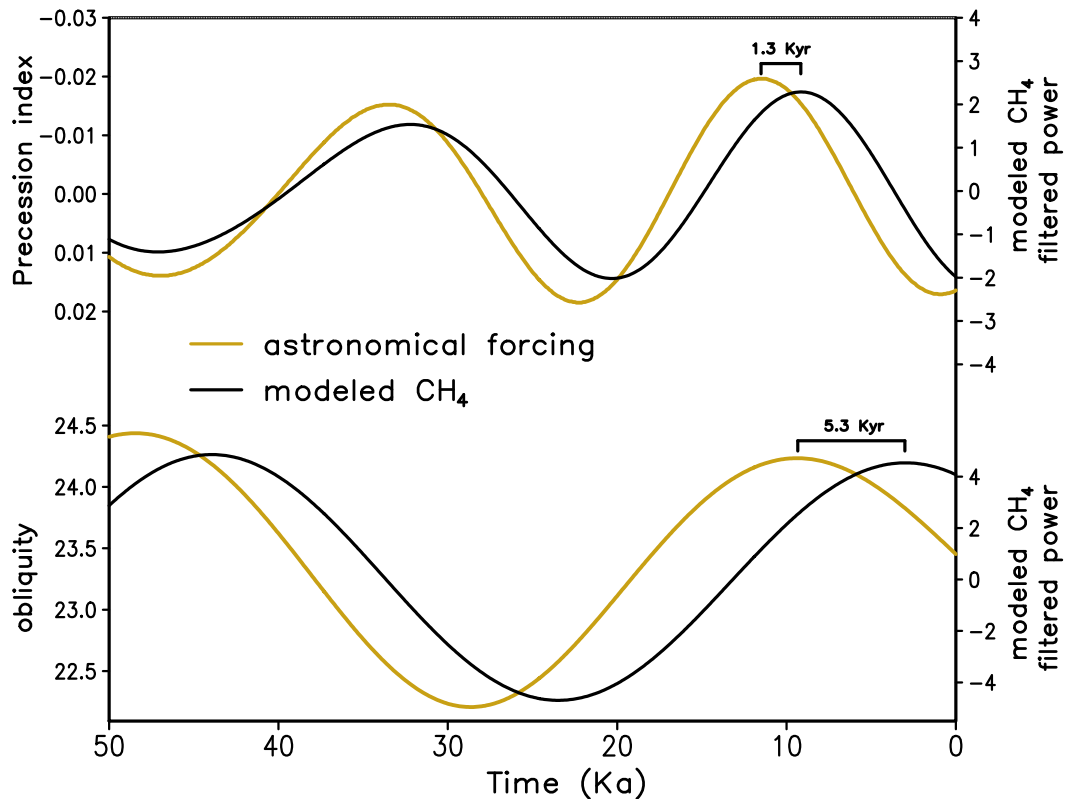


**Fig. 8.** Top: TRENCH simulated global CH<sub>4</sub> emissions, band pass filtered for 21 kyr ( $\pm 2.5$  kyr) and the precession index, and (bottom) TRENCH simulated global CH<sub>4</sub> emissions, band pass filtered at 41 k ( $\pm 3$  kyr), and the obliquity parameter. Lags between forcing and response are indicated for each timescale.



## Methane variations on orbital timescales: a transient modeling experiment

T. Y. M. Konijnendijk et al.

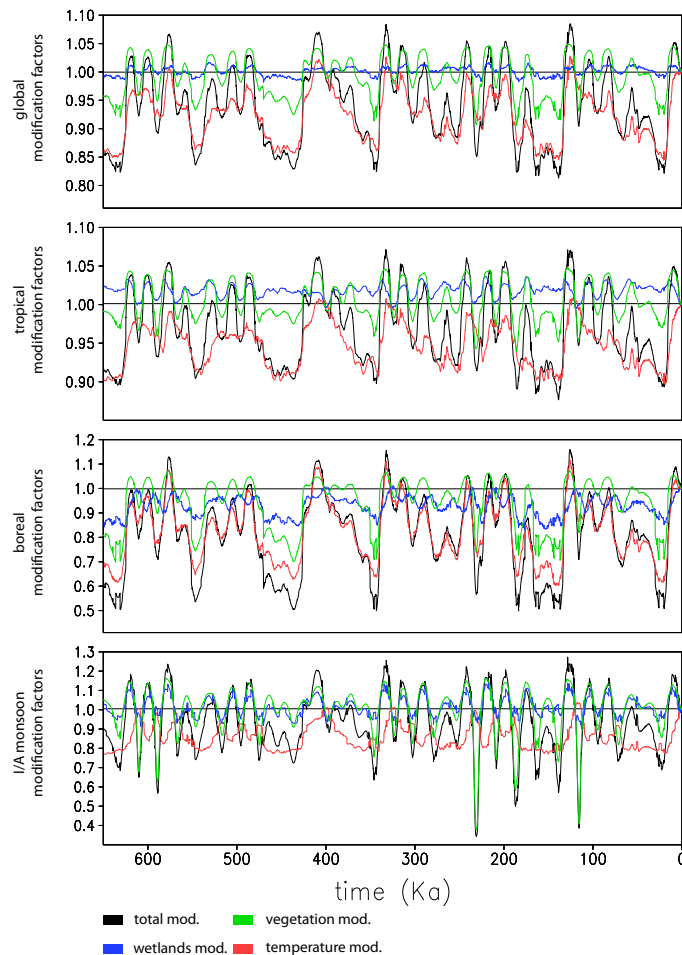


**Fig. 9.** Time series of the modification factors, as defined in Sect. 3.2, for the entire globe and for the tropical, boreal and Indian/Asian monsoon areas separately.

Title Page

Abstract

Introduction

Conclusions

References

Tables

Figures

◀

▶

◀

▶

Back

Close

Full Screen / Esc

Printer-friendly Version

Interactive Discussion

## Methane variations on orbital timescales: a transient modeling experiment

T. Y. M. Konijnendijk et al.

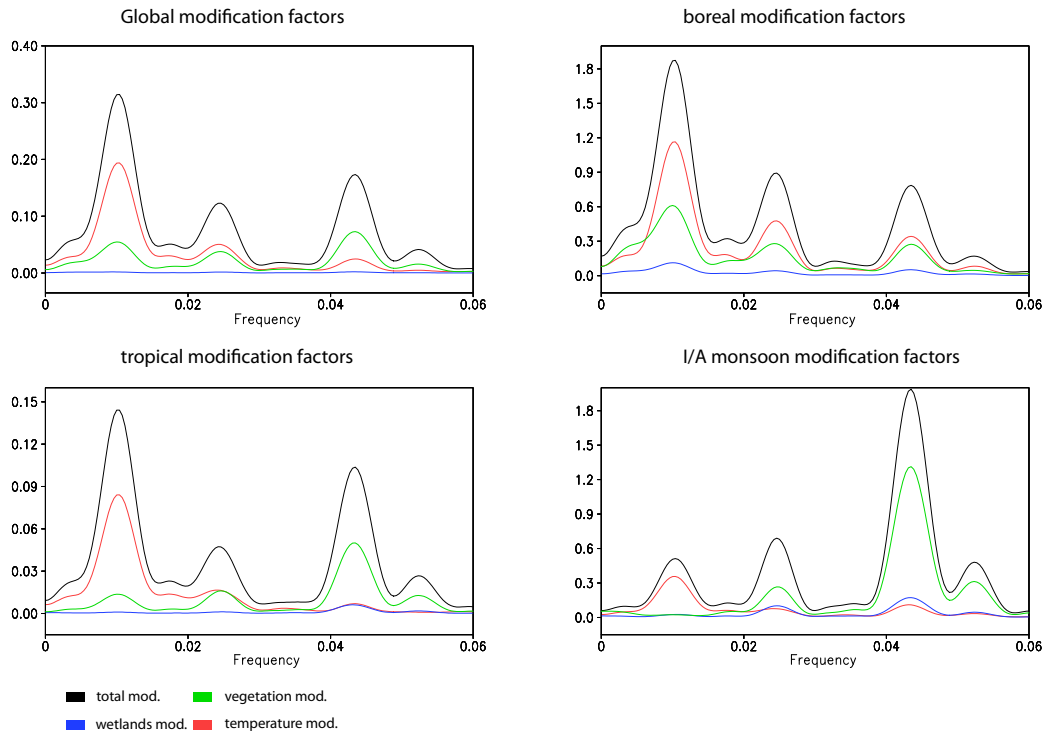


**Fig. 10.** Spectra of the modification factors (see Sect. 3.2) for the entire globe, and for the tropical, boreal and Indian/Asian monsoon areas separately.